Proceedings of the 21st ICSMGE, Vienna, Austria, 14 – 19 June 2026. Pistrol, Adam & Schweiger (eds.)
Published by: ÖGG, Austrian Society for Geomechanics, Salzburg, Austria, ISBN 978-3-9503898-4-5
https://doi.org/10.53243/ICSMGE2026-1588

Geometric-learning-enabled data-driven discovery of interpretable water retention models for deformable porous media

Yejin Kim, Hyoung Suk Suh
Department of Civil and Environmental Engineering, Case Western Reserve University, Cleveland, United States
hssuh@case.edu

Jinhyun Choo
Department of Civil and Environmental Engineering, Seoul National University, Seoul, South Korea

ABSTRACT: The water retention behavior of porous media is a key factor controlling unsaturated flow, and is strongly influenced by deformation of the solid matrix. However, accurately modeling this behavior—while explicitly accounting for its dependence on deformation and preserving interpretability—remains a significant challenge. In this work, we present a data-driven framework that can automatically discover interpretable models for the water retention behavior of deformable porous materials, achieving predictive accuracy comparable to conventional black-box machine learning approaches. Our approach employs a geometric learning approach based on physics-constrained symbolic regression, which incorporates monotonicity constraints derived from physical principles to generate mathematical expressions directly from datasets produced by image-based pore-scale flow simulations. The discovered models are validated against simulation results that are not included in the training dataset, demonstrating both accuracy and physical consistency. Further, the explicit mathematical form of the proposed model facilitates seamless integration into continuum-scale simulations, providing a practical and efficient means to capture multi-scale processes in unsaturated flow without incurring computational costs.

KEYWORDS: Physics-constrained geometric learning, Interpretable machine learning, Symbolic regression, Water retention model.

1 INTRODUCTION

The water retention behavior of porous materials can be characterized by the relationship between matric suction and saturation level, as it serves as a descriptor for understanding and predicting multiphase fluid flow in unsaturated media. This suction-saturation relation can be obtained either from experiments or from pore-scale simulations, including image-based methods (e.g., Dong and Blunt, 2009; Suh et al., 2017; Chadwick et al., 2022; Kim and Suh, 2025).

Standard water retention models, including the van Genuchten, Brooks–Corey, and Fredlund–Xing equations (Brooks and Corey, 1964; van Genuchten, 1980; Fredlund and Xing, 1994) provide closed-form mathematical expressions with adjustable parameters that can be calibrated to fit the data. Although these models are widely used in practice, their fixed functional forms often restrict their ability to represent complex retention behaviors, particularly in deformable porous media where changes in pore size and geometry under stress or fluid pressure result in highly nonlinear responses.

Such limitations motivate the need for more flexible, data-driven approaches capable of automatically identifying functional forms from data while preserving the model's interpretability. Symbolic regression offers a promising framework for discovering mathematical expressions directly from data without prescribing the equation form in advance (Cranmer et al., 2020; Suh et al., 2024a). However, purely data-driven symbolic regression may yield expressions that violate fundamental physical principles or exhibit unrealistic behavior beyond the range of the fitted data. To address these issues, we incorporate physics-based geometric constraints into the symbolic regression process, ensuring that the discovered expressions remain physically consistent while retaining the flexibility to capture complex retention behaviors. Compared to the two-stage hybrid approach proposed in Suh et al. (2024a) that relies on a sequential "neural network + symbolic regression" pipeline, the present method directly extracts a closed-form symbolic regression from the dataset in a single step. This direct formulation eliminates the need for neural network pre-training and enables a more transparent, interpretable discovery process.

The objective of this study is to leverage an interpretable machine learning approach for directly discovering mathematical expressions that describe the water retention behavior of deformable porous media. Specifically, we apply symbolic regression directly to datasets obtained from image-based pore-scale drainage simulations and incorporate monotonicity constraints to improve accuracy and physical consistency. The resulting expressions provide concise and interpretable representations of the underlying pore-scale behavior, enabling reliable prediction of water retention curves for both seen and unseen microstructures within and beyond the training range. In this work, we focus exclusively on drainage processes and do not consider hysteresis effects.

2 METHODOLOGY

This section begins by describing the image-based method used to generate water retention data from digital microstructures (Section 2.1). Next, we introduce the proposed physics-constrained symbolic regression framework, which leverages these simulation data to discover concise and interpretable mathematical expressions that can describe the geometry of the water retention model for deformable porous materials that are physically consistent (Section 2.2).

2.1 *Image-based two-phase flow simulations*

In this study, we employed an image-based sphere insertion method (Hilpert and Miller, 2001; Suh et al., 2024b) to simulate drainage in digital representations of porous materials and to generate water retention data. The method begins with a binary image of the porous medium, obtained from either two-dimensional or three-dimensional digital image data. In this binary image, voxels (or pixels) assigned a value of 0 represent the solid phase, while those with a value of 1 correspond to the pore space. A Euclidean distance transform is then applied to the pore space to produce a distance map, where each voxel value corresponds to the radius of the largest sphere that can be inscribed therein. Through the Young–Laplace equation, i.e.,

$$p_c = \frac{2\gamma_{aw}\cos\theta}{r}, \quad (1)$$

this radius map is converted into the minimum capillary pressure required to invade each pore region. Here, γ_{aw} denotes the air-water interfacial tension, θ is the contact angle, and r is the effective inscribed-sphere radius. This means that we can determine, for each voxel, whether it has been invaded by the non-wetting fluid based on a series of morphological operations. When a specific value of suction s is given, a binary mask can be generated by applying the threshold $r_{th} = 2\gamma_{aw}\cos\theta/s$. This mask represents the regions that can be considered invaded by the non-wetting fluid, namely those where the minimum capillary pressure needed for invasion is less than or equal to s. However, the binary mask may include voxels with a minimum capillary pressure below s that are identified as invaded but are not connected to the inlet face. These isolated regions are excluded by retaining only those voxels that form continuous pathways from the inlet, so that the computed invaded volume represents only the pore space that can be physically reached at the given suction. These connected voxels are then expanded by a morphological dilation with radius r_{th}, providing an approximation of the fluid configuration at that suction. The degree of saturation S_w is computed as the fraction of the pore volume that remains water-filled. By progressively increasing s and repeating the procedure, we obtain a set of (s, S_w) pairs that form a discrete water retention curve, analogous to the outcome of a quasi-static drainage experiment.

In this work, we generated multiple representative digital microstructures designed to emulate a porous medium subjected to isotropic confinement. For each microstructure, an image-based pore-scale drainage simulation was performed, producing a set of $\{v^i, s^i, S_w^i\}_{i=1}^{N_{\text{data}}}$, where $v = 1 + e$ is the specific volume, e is the void ratio, and N_{data} denotes the total number of data points along a single water retention curve. The combined dataset forms a continuous surface in a three-dimensional Euclidean space that characterizes the water retention behavior of deformable porous media. Details of the generated microstructures and the corresponding simulation results are presented in Section 3.1.

2.2 *Physics-constrained symbolic regression*

This section outlines the procedure for constructing a geometric representation, i.e., a water retention model, from a point cloud $\{v^i, s^i, S_w^i\}_{i=1}^{N_{\text{data}}}$ generated in Section 2.1. While a multilayer perceptron and other neural-network-based models can, in principle, be trained to approximate the mapping between inputs and outputs, these approaches often suffer from overfitting when the available dataset is limited, and their inherent black-box nature significantly limits interpretability, making it challenging to extract meaningful insights from the learned functions (Bahmani et al., 2024; Suh et al., 2024a).

For these reasons, we adopt symbolic regression, which searches for an explicit mathematical expression that is both predictive and interpretable. This work employs genetic programming for symbolic regression, where each candidate mathematical expression is represented as a binary tree whose internal nodes correspond to mathematical operators and leaves represent variables or constants (McConaghy, 2011; Cranmer et al., 2020). The operator set includes common binary operators, such as $+$, $-$, and $\times$, as well as unary operators such as $\exp(\cdot)$, $\sin(\cdot)$, and $\cos(\cdot)$. The algorithm evolves an initial population of random expressions through selection, crossover, and mutation operations guided by a fitness function that balances predictive accuracy with model complexity. This search strategy bypasses the need to predefine an explicit mathematical form and enables the data-driven discovery of relationships among specific volume, suction, and degree of saturation.

Our objective is to identify a symbolic expression $f^{\text{PCSR}}(v, s)$ that predicts the degree of saturation S_w for a given specific volume v and suction s. To ensure that the discovered expressions adhere to established physical behavior in drainage processes, we impose two monotonicity constraints: S_w must be a monotonically decreasing function of matric suction s, and S_w must be a monotonically decreasing function of specific volume v. These conditions are incorporated into the learning problem as a physics loss, combined with the data loss, leading to the following learning objective:

$$L = L_{\text{data}} + L_{\text{phys}}. \quad (2)$$

Here, the data loss (L_{data}) term is given by

$$L_{\text{data}} = \frac{1}{N_{\text{data}}} \sum_{i=1}^{N_{\text{data}}} \left[f^{\text{PCSR}}(v^i, s^i) - S_w^i \right]^2, \quad (3)$$

which is the mean squared error between the predicted values from f^{PCSR} and the data, while f^{PCSR} denotes the function discovered via the physics-constrained symbolic regression. The physics loss (L_{phys}) enforces the monotonicity constraints:

$$L_{\text{phys}} = \frac{1}{N_{\text{data}}} \sum_{x \in \{v,s\}} \sum_{i=1}^{N_{\text{data}}} \left[\max\left(0, \frac{\partial S_w}{\partial x}\Big|_{(v^i, s^i)}\right)\right]^2, \quad (4)$$

where $\partial S_w / \partial x$ indicates the partial derivative of the degree of saturation S_w with respect to the input variable $x \in \{v, s\}$. Since S_w is required to be monotonically decreasing with respect to both v and s, any positive values of derivatives indicate the violation of monotonicity constraints.

Figure 1 presents a schematic of the proposed physics-constrained symbolic regression framework applied to the data collected from pore-scale simulations. Here, a superposed tilde is used to indicate the saturation predicted by the discovered symbolic expression. The framework maintains the predictive capability of black-box machine learning models, while it provides a closed-form equation that is inherently human-interpretable. This not only enhances the trustworthiness of the learned function but also improves its portability by enabling seamless integration into existing continuum-scale partial differential equation solvers.

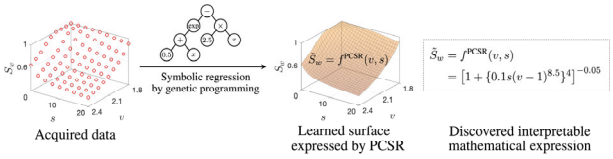

Figure 1. Schematic of the physics-constrained symbolic regression approach applied directly to image-based pore-scale drainage simulations to discover interpretable water retention models.

Beyond these advantages, the proposed framework demonstrates how symbolic regression can be systematically augmented with physics-based constraints to suppress non-physical behavior during training. Because each candidate model is represented as an explicit mathematical expression, the required physical trends, such as the monotonic decrease of saturation with respect to suction and specific volume, can be evaluated directly on the expression and incorporated into the learning objective. This prevents unrealistic functional shapes from emerging during the evolutionary search and guides the optimization toward expressions that remain physically admissible by construction. As a result, the discovered models not only fit the data but also exhibit the qualitative behavior expected for unsaturated porous materials, providing a principled and extensible foundation for uncovering

interpretable constitutive relationships. The results will be presented and discussed in great detail in Section 3.2.

3 RESULTS AND DISCUSSION

This section begins by presenting the results of image-based pore-scale simulations conducted on a series of randomly generated digital microstructures, which form the dataset for the proposed geometric learning framework. Section 3.1 provides a detailed account of the microstructure generation process, designed to replicate snapshots of a porous medium under isotropic confinement, and describes the corresponding discrete water retention curves obtained from the simulations. Based on this dataset, Section 3.2 applies the physics-constrained symbolic regression framework introduced in Section 2.2, focusing on the discovery of concise, interpretable mathematical expressions for water retention behavior and assessing their predictive capability. All image-based simulations were performed using the PoreSpy image analysis toolkit (Gostick et al., 2019), and the symbolic regression models were implemented with PySR (Cranmer, 2023) in combination with PyTorch (Paszke et al., 2019).

3.1 *Image-based drainage simulations in deforming porous material*

In this study, a series of synthetic digital microstructures was generated to represent volumetric elements of a deformable porous medium under different isotropic confinement conditions. Each microstructure was represented as a 500 × 500 × 500 voxel domain with a spatial resolution of 2 μm/voxel. The structures were obtained by first generating a random binary field of pore and solid phases following the procedure of Ávila et al. (2022), applying a Gaussian blur with a blobiness parameter of 1.5, and then thresholding the blurred field to achieve the desired specific volume v. The target values of v ranged from 1.8 to 2.4 in increments of 0.05, resulting in 13 distinct configurations. Figure 2 presents an exemplary digital microstructure with $v = 2.4$, and a snapshot from the drainage simulation taken at $S_w = 0.986$.

Following the methodology outlined in Section 2.1, each microstructure was subjected to image-based pore-scale drainage simulations using the sphere insertion approach. In all simulations, the air–water interfacial tension was set to $\gamma_{aw} = 0.072\ \mathrm{N/m}$ and the contact angle to $\theta = 0$. The pore water pressure was fixed at $p_w = 0$ at the top boundary ($z = L_z$), while the suction $s = p_a - p_w$ was increased from 0 kPa to 20 kPa with a 1 kPa interval. At each increment, the corresponding degree of saturation S_w was recorded, producing a discrete water retention curve for the given microstructure. As hinted in Figure 3, these curves consist of measurements that consistently reflect trends in water retention behavior concerning both suction and specific volume, supporting the assumption that the generated microstructures can be considered a single material type. Moreover, these observations motivate the development of a phenomenological model capable of describing the specific volume-suction-saturation relationship, which can be either formulated analytically or discovered through data-driven techniques, such as the physics-constrained symbolic regression framework proposed in this work.

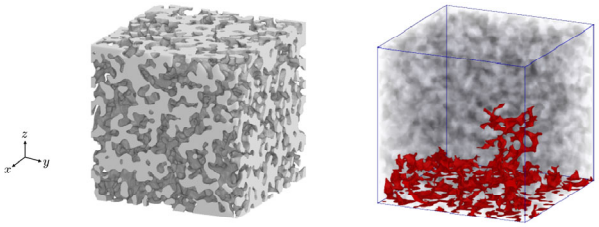

$v = 2.4$ $S_w = 0.986$

Figure 2. Representative digital microstructure with a specific volume of $v = 2.4$ and a snapshot from the image-based drainage simulation illustrating non-wetting phase invasion.

3.2 *Data-driven discovery of water retention models using physics-constrained symbolic regression*

Using the water retention dataset generated from the pore-scale simulations, our goal is to identify an interpretable, data-driven model for the target porous material using physics-constrained symbolic regression. As previously discussed, the simulation results are represented as point clouds $\{v, s, S_w\}$ in a three-dimensional Euclidean space, which serve as the training data for constructing an optimal geometric object that can be defined explicitly through a symbolic expression. In principle, if the dataset is generated from a known function and the set of allowable operators is appropriately defined, the symbolic regression approach can discover an expression that closely matches the benchmark. In the absence of any prior knowledge about the exact function, we specified the unary operator set for training as $\{\mathrm{abs}(\cdot), \exp(\cdot), \mathrm{sqrt}(\cdot), \mathrm{inv}(\cdot)\}$ and the binary operator set as $\{+, -, \times, \div, \hat{}\}$, where $\mathrm{abs}(\cdot) = |\cdot|, \mathrm{sqrt}(\cdot) = \sqrt{\cdot}$, $\mathrm{inv}(\cdot) = 1/\cdot$, with the symbol $'\hat{}'$ denoting the power operation. The symbolic regression was executed for 1,000 iterations, with 15 populations evaluated in each iteration. Each population consists of 33 individual binary trees, and the maximum allowed size for any expression tree was set to 40 nodes, which represents the highest complexity level allowed.

To ensure that the discovered expressions remained physically meaningful throughout training, the monotonicity constraints described in Section 2.2 were evaluated at every evolutionary step using automatic differentiation. For each candidate expression, the partial derivatives $\partial S_w/\partial v$ and $\partial S_w/\partial s$ were computed directly from the symbolic tree, and any violation of the required decreasing trends was penalized through the physics loss term. This mechanism prevented candidate expressions that violated the required monotonic trends from surviving in the evolutionary process. Training continued until the combined loss, $L_{\mathrm{data}} + L_{\mathrm{phys}}$, reached a stable and sufficiently low value, indicating both a good fit to the reference data and strict adherence to the imposed physical constraints.

Figure 3 presents the geometric object learned from the data, using the proposed framework. The green surface corresponds to the mathematical expression discovered by the trained model, while the hollow symbols represent the reference data from the image-based simulations. The surface closely matches the simulation points across the domain, reproducing the expected monotonic variation of S_w with respect to both v and s.

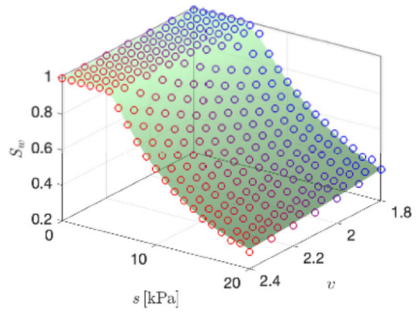

Figure 3. Surface representations obtained from the proposed physics-constrained symbolic regression model. The green surface depicts the discovered mathematical expression, while hollow symbols represent the corresponding image-based simulation results, which serve as the reference data for comparison.

The explicit expressions discovered by the physics-constrained symbolic regression framework at different complexity levels are presented in Figure 4, together with their corresponding total loss [Equation (2)]. Expressions with a lower complexity level yield more compact expressions, but may result in higher predictive errors, whereas higher-complexity models better fit the reference data.

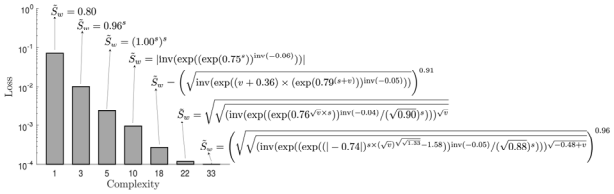

Figure 4. Discovered symbolic expressions across different complexity levels obtained from the physics-constrained symbolic regression model, along with their computed losses.

To demonstrate the predictive capability of the discovered expressions, additional image-based drainage simulations were conducted on two digital microstructures that were not included in the training dataset. For benchmarking purposes, a black-box neural network model and a vanilla symbolic regression model were also trained on the same dataset, and their predictions for the unseen microstructures were compared. All parameters for microstructure generation were identical to those specified in Section 2.1. For the interpolation scenario, illustrated in the top plot of Figure 5, a specific volume of $v = 1.825$ was selected, placing it within the range of values included in the training dataset. Conversely, the extrapolation scenario, shown in the right plot of Figure 5, utilized a specific volume of $v = 2.5$ that lies outside the bounds of the training data. In each plot, black hollow symbols represent the image-based simulation data, the yellow dashed line corresponds to the neural network model, the green dotted line to the vanilla symbolic regression model, and the red solid line to the best-fit symbolic expression obtained from the proposed framework.

At the global scale, the interpolation case ($v = 1.825$) shows that both the NN and the PCSR expression closely follow the reference simulation data, whereas the vanilla SR model begins to deviate below the air-entry value. In the extrapolation case ($v = 2.5$), the predictive accuracy of all models decreases relative to the interpolation scenario, yet both the NN and the PCSR expression still capture the overall decreasing trend. The vanilla SR model, however, exhibits noticeable departures from the reference behavior at low suctions. Although the global plots in Figure 5 provide an overall comparison among the three models, the air-entry region spans only a narrow portion of the curve, which visually compresses the physically relevant curvature changes associated with the onset of drainage.

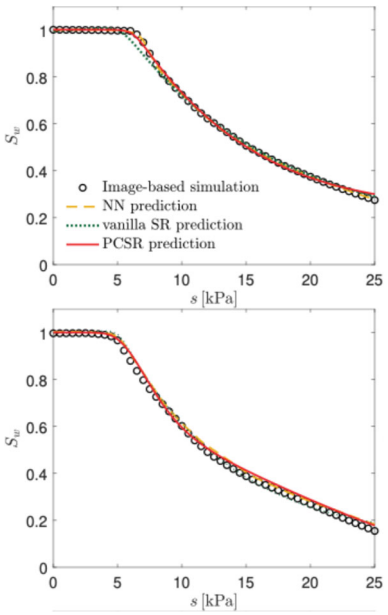

Figure 5. Predicted water retention curves for unseen digital microstructures: interpolation case with v = 1.825 (top) and extrapolation case with v = 2.5 (bottom).

To more clearly examine these differences, the air-entry segments of both cases are magnified in Figure 6, allowing detailed inspection of the model behavior in this physically sensitive region. In the interpolation scenario at $v = 1.825$, the magnified view in Figure 6 (top) shows that the NN prediction exhibits several rapid curvature changes near the air-entry point, a symptom of overfitting to the discrete training data. This oscillatory response is undesirable for water retention modeling because the air-entry region provides the key slope information used to extract hydraulic parameters, and overfitting in this part of the curve prevents their reliable estimation. In contrast, the proposed PCSR approach produces a smooth transition that remains consistent with the underlying physical expectation. For the extrapolation case at $v = 2.5$, the enlarged segment in Figure 6 (bottom) illustrates that the vanilla SR model violates monotonicity by exhibiting a locally increasing slope at low suctions, whereas the PCSR expression maintains the required decreasing trend. This demonstrates that the physics loss introduced within the proposed PCSR framework effectively suppresses monotonicity violations, enabling the discovered expression to retain a physically reasonable decreasing trend even outside the range of the training data.

In practical multi-scale applications, the symbolic expression discovered by the PCSR framework, $f^{\mathrm{PCSR}}(v, s)$, can serve as a data-driven surrogate for conventional empirical water-retention models. Whereas empirical formulations require parameter calibration to prescribed functional forms, the PCSR-based approach derives an interpretable closed-form relation directly from data without imposing any prior equation structure. This property allows the learned expression to be incorporated into continuum-scale finite element analyses in a straightforward manner, providing a physically interpretable constitutive relation for unsaturated flow modeling.

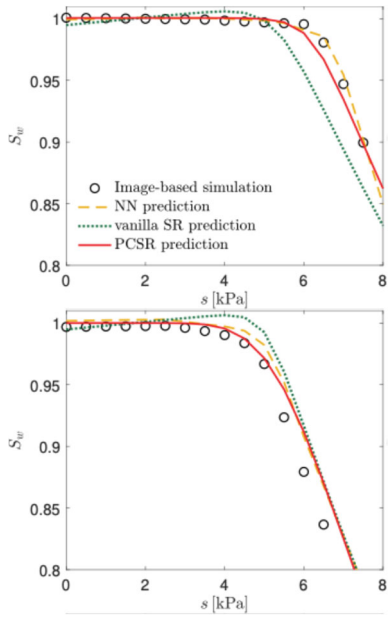

Figure 6. Magnified air-entry region for unseen digital microstructures: interpolation case with v = 1.825 (top) and extrapolation case with v = 2.5 (bottom).

The present study focuses on the methodological development and proof-of-concept demonstration of the proposed physics-constrained symbolic regression framework using numerically generated pore-scale datasets obtained from image-based drainage simulations. Accordingly, the objective here is to assess the feasibility, interpretability, and physical consistency of the discovered expressions against numerically constructed benchmarks, rather than to benchmark the method against experimentally measured water retention curves. Future work will extend this framework to experimentally acquired datasets to further evaluate its predictive capability under real material conditions.

4 CONCLUSIONS

In this study, we introduced a data-driven geometric learning framework for developing interpretable models of water retention behavior in deformable porous media. By integrating symbolic regression with physics constraints, our approach achieves both high predictive accuracy and interpretability. The framework was rigorously validated using datasets generated from image-based drainage simulations at the pore scale, which capture the essential features of water retention in deformable porous materials. Unlike conventional black-box neural networks, the proposed method produces symbolic expressions that retain physical consistency by enforcing monotonicity constraints during training. When evaluated on digital microstructures outside the training dataset, the physics-constrained symbolic regression model accurately reproduced water-retention curves, performing comparably to the benchmark neural network model. Furthermore, the physics-constrained symbolic regression model delivers its predictions in the form of explicit mathematical equations, facilitating seamless integration into continuum-scale numerical solvers. With its combination of interpretability, physical consistency, and portability, the proposed framework is expected to serve as a robust and practical tool for multi-scale simulation of unsaturated flow in deformable porous media.

Beyond its demonstrated performance on image-based pore-scale datasets, the proposed PCSR framework provides a versatile foundation for constitutive modeling of unsaturated geomaterials. Because the resulting expression is explicit and closed-form, it can be directly embedded into continuum-scale finite-element formulations for unsaturated flow or hydro-mechanical analysis without requiring surrogate neural networks or iterative parameter calibration. This interpretability makes the method particularly attractive for multi-scale workflows in which pore-scale morphology, drainage characteristics, and continuum-scale response must be connected in a transparent manner. In addition, the framework extends the capability of symbolic regression itself by incorporating physics-based constraints directly into the search process. Rather than relying solely on statistical fitting, the method enforces physically meaningful behavior during training, preventing the emergence of non-physical trends that commonly arise in unconstrained data-driven models. This demonstrates that domain knowledge can be encoded as mathematically enforceable constraints within the symbolic discovery procedure, enabling the resulting expressions to remain aligned with the intended physical behavior while preserving the interpretability inherent to closed-form formulations.

While the present study focused on numerically generated microstructures to isolate and evaluate the core methodology, extending the PCSR approach to experimentally measured water retention data remains an important direction for future research. Nevertheless, the findings demonstrate that physics-constrained symbolic regression can provide physically consistent and interpretable closed-form relationships, offering a promising foundation for future integration into large-scale numerical analyses and practical multi-scale geotechnical applications.

5 ACKNOWLEDGEMENTS

This work was supported by the National Research Foundation of Korea (NRF) grant funded by the Korea government (MSIT) (No. RS-2024-00360509), and the start-up grant from Case Western Reserve University.

6 REFERENCES

Ávila, J., Pagalo, J. and Espinoza-Andaluz, M., 2022. Evaluation of geometric tortuosity for 3D digitally generated porous media considering the pore size distribution and the A-star algorithm. Scientific Reports, 12(1). https://doi.org/10.1038/s41598-022-23643-6.

Bahmani, B., Suh, H.S. and Sun, W., 2024. Discovering interpretable elastoplasticity models via the neural polynomial method enabled symbolic regressions. Computer Methods in Applied Mechanics and Engineering, 422, p.116827.

Brooks, R. and Corey, T., 1964. Hydraulic properties of porous media. Colorado State University.

Chadwick, E.A., Hammen, L.H., Schulz, V.P., Bazylak, A., Ioannidis, M.A. and Gostick, J.T., 2022. Incorporating the effect of gravity into image-based drainage simulations on volumetric images of porous media. Water Resources Research, 58(3), p.e2021WR031509.

Cranmer, M., 2023. Interpretable machine learning for science with PySR and SymbolicRegression. jl. arXiv preprint arXiv:2305.01582.

Cranmer, M., Sanchez Gonzalez, A., Battaglia, P., Xu, R., Cranmer, K., Spergel, D. and Ho, S., 2020. Discovering symbolic models from deep learning with inductive biases. Advances in neural information processing systems, 33, pp.17429-17442.

Dong, H. and Blunt, M.J., 2009. Pore-network extraction from micro-computerized-tomography images. Physical Review E—Statistical, Nonlinear, and Soft Matter Physics, 80(3), p.036307.

Fredlund, D.G. and Xing, A., 1994. Equations for the soil-water characteristic curve. Canadian geotechnical journal, 31(4), pp.521–532.

van Genuchten, M.T., 1980. A closed-form equation for predicting the hydraulic conductivity of unsaturated soils. Soil science society of America journal, 44(5), pp.892–898.

Gostick, J.T., Khan, Z.A., Tranter, T.G., Kok, M.D., Agnaou, M., Sadeghi, M. and Jervis, R., 2019. PoreSpy: A python toolkit for quantitative analysis of porous media images. Journal of Open Source Software, 4(37), p.1296.

Hilpert, M. and Miller, C.T., 2001. Pore-morphology-based simulation of drainage in totally wetting porous media. Advances in water resources, 24(3-4), pp.243-255.

Kim, Y. and Suh, H.S., 2025. GNPNM: A graph neural pore network model for predicting quasi-static drainage displacement patterns. Computers and Geotechnics, 187, p.107497.

McConaghy, T., 2011. FFX: Fast, scalable, deterministic symbolic regression technology. Genetic Programming Theory and Practice IX.

Paszke, A., Gross, S., Massa, F., Lerer, A., Bradbury Google, J., Chanan, G., Killeen, T., Lin, Z., Gimelshein, N., Antiga, L., Desmaison, A., Xamla, A.K., Yang, E., Devito, Z., Raison Nabla, M., Tejani, A., Chilamkurthy, S., Ai, Q., Steiner, B., Facebook, L.F., Facebook, J.B. and Chintala, S., 2019. PyTorch: An Imperative Style, High-Performance Deep Learning Library.

Suh, H.S., Kang, D.H., Jang, J., Kim, K.Y. and Yun, T.S., 2017. Capillary pressure at irregularly shaped pore throats: Implications for water retention characteristics. Advances in Water Resources, 110, pp.51-58.

Suh, H.S., Song, J.Y., Kim, Y., Yu, X. and Choo, J., 2024a. Data-driven discovery of interpretable water retention models for deformable porous media. Acta Geotechnica, 19(6), pp.3821-3835.

Suh, H.S., Na, S. and Choo, J., 2024b. Pore-morphology-based estimation of the freezing characteristic curve of water-saturated porous media. Water Resources Research, 60(8), p.e2024WR037035.